Colombiamar 2019

VI Congreso Internacional de
DISEÑO E INGENIERÍA NAVAL

COPINAVAL

XXVI
CONGRESO PANAMERICANO DE INGENIERÍA NAVAL, TRANSPORTE MARÍTIMO E INGENIERÍA PORTUARIA

Organizan

COTECMAR

ESCUELA NAVAL ALMIRANTE PADILLA

INSTITUTO PANAMERICANO DE INGENIERIA NAVAL

Hydrodynamic Analysis of Inland Vessel Self-Propulsion for Cargo Transport for Navigability in the Magdalena River

Oscar D. Acosta Lopera [1]

Kazuo Nishimoto [1]

Jairo H. Cabrera Tovar [2]

1. Numerical Offshore Tank (TPN), Department of Naval and Oceanic Engineering (PNV), Polytechnic School (EP), The University of São Paulo (USP), São Paulo (São Paulo), Brazil.
2. Department of Naval Engineering, Faculty of Engineering, The Technological of Bolivar University (UTB), Cartagena (Bolivar), Colombia.

Content

1. Introduction
2. Ship geometry
3. Numerical model
4. Empirical models
5. Methodology
6. Results
7. Conclusions and future works

Content

1. Introduction

The objective of this work is the study of the resistance of a 2700 DWT self-propelled inland vessel by numerical simulation. The numerical results are compared to the existing empirical formulas and the experimental test results being, therefore, validated.

Content

1. Introduction
2. Ship geometry
3. Numerical model
4. Empirical models
5. Methodology
6. Results
7. Conclusions and future works

2. Ship geometry

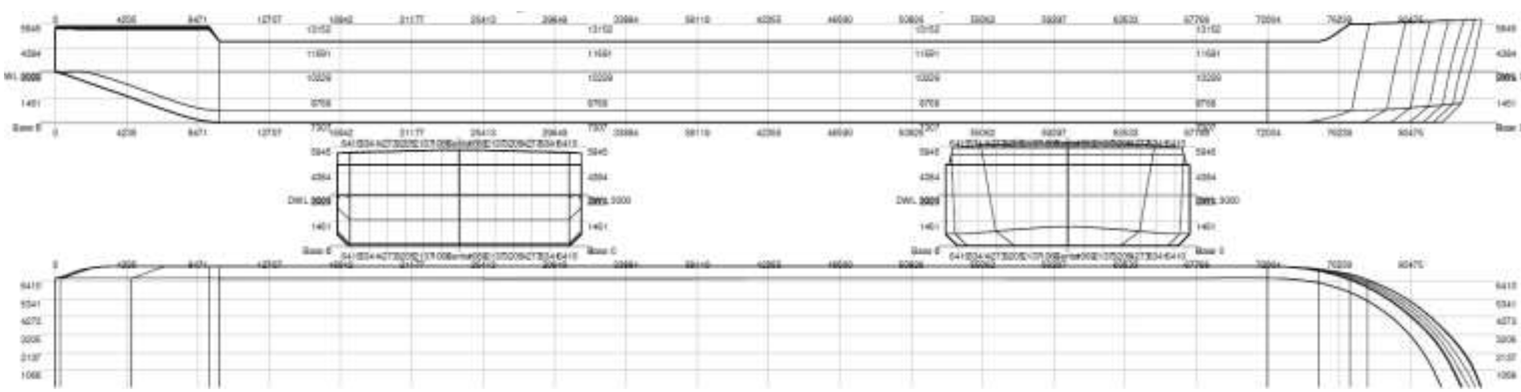

Fig. 1. Lines-plan of the self-propelled inland vessel.

Particulars	Full scale	Model scale
Length between perpendiculars L_{pp}(m)	83.86	4.193
Breadth B (m)	14.50	0.725
Design draft T (m)	3.20	0.160
Wet surface area S_{ws} (m^2)	1564.40	3.911
Displacement Λ (m^3)	3560.00	0.445

Table 1. Main particulars of the 2700 DWT inland vessel.

Content

1. Introduction
2. Ship geometry
3. Numerical model
4. Empirical models
5. Methodology
6. Results
7. Conclusions and future works

3. Numerical model

RANS equation

$$\frac{\partial \rho}{\partial t} + \frac{\partial}{\partial x_j}(\rho U_i) = 0, \tag{1}$$

$$\frac{\partial}{\partial t}(\rho U_i) + \frac{\partial}{\partial x_j}(\rho U_i U_j) = -\frac{\partial P}{\partial x_i} + \frac{\partial}{\partial x_j}\left[\mu\left(\frac{\partial U_i}{\partial x_j} + \frac{\partial U_j}{\partial x_i} - \frac{2}{3}\delta_{ij}\frac{\partial U_i}{\partial x_i}\right)\right] + \frac{\partial}{\partial x_j}\left(-\rho\overline{u'_i u'_j}\right) \tag{2}$$

$$\rho = \sum_{n=1}^{2} \alpha_n \rho_n \,, \qquad \mu = \sum_{n=1}^{2} \alpha_n \mu_n \,, \tag{3}$$

where $x_{i,j}$ $(i,j = 1,2,3,\ i \neq j)$ are the components of Cartesian coordinates, $U_{i,j}$ $(i,j = 1,2,3,\ i \neq j)$ are the mean velocity components, P is the mean pressure, μ is the viscosity, δ_{ij} is the delta Kronecker and $-\rho u'_i u'_j$ is the Reynolds stress tensor.

3. Numerical model

For the numerical solution of the viscous flow, the CDF software STAR-CCM+ is applied to the RANS equation solution. The Finite Volume Methods (FVM) is used to the discretization of the computational domain in a Volume Control (VC). The k-ε turbulence model is used to describe the fluid motion in turbulent state. To tracking and locating the free surface, Volume of the Fluid (VOF) is applied.

3. Numerical model

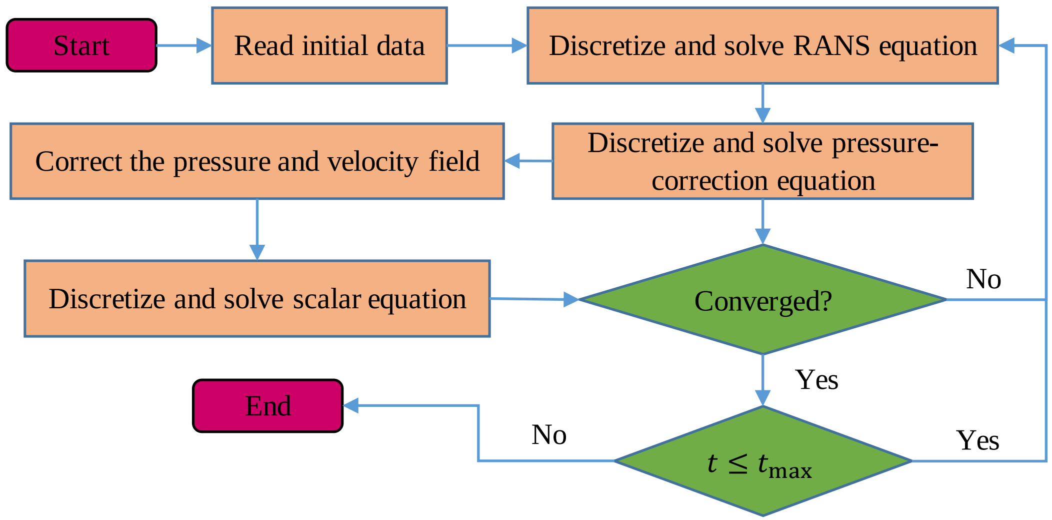

Fig. 2. Main flow chart in the STAR-CCM+ solver.

3. Numerical model

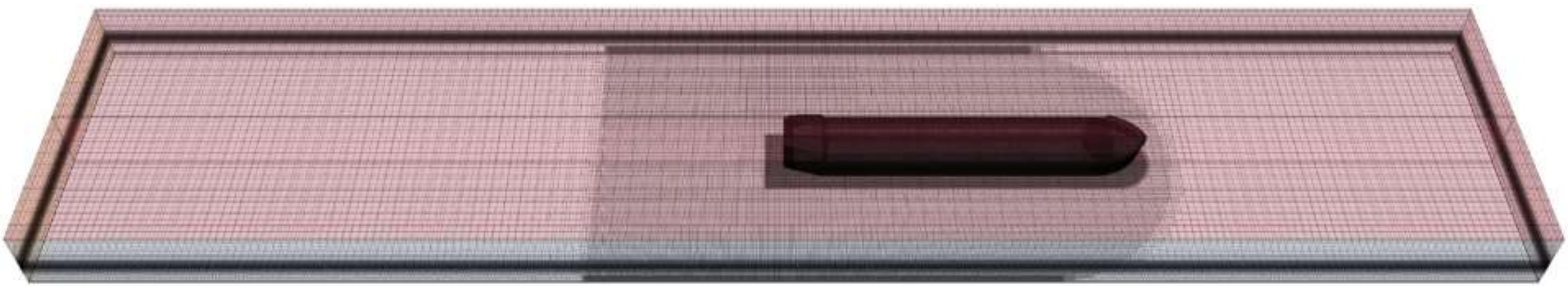

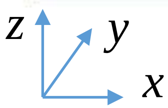

Fig. 3. Overview of the computational domain.

Total elements: 8,307,654.

Free surface zone refinement: x and y axes with 2.12498e-2 m; z with 2.65625E-3 m.

	L	Domain dimensions (m)
Length	1.00	4.24
Back	1.98	8.40
Front	0.98	4.16
Side	0.41	1.75
Height	0.19	0.80

Table. 2. Geometry dimensions in the computational domain.

3. Numerical model

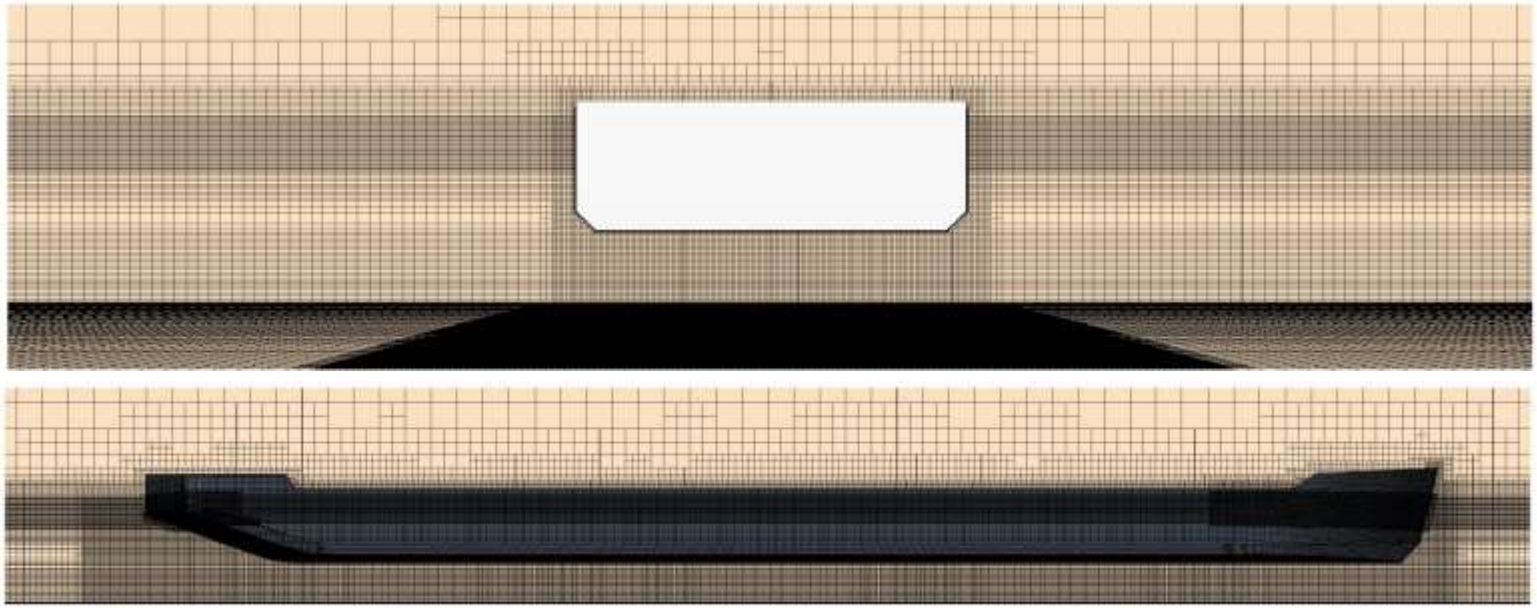

Fig. 4. . Grid structure around the vessel. Top, midship section; bottom, longitudinal section at symmetry.

3. Numerical model

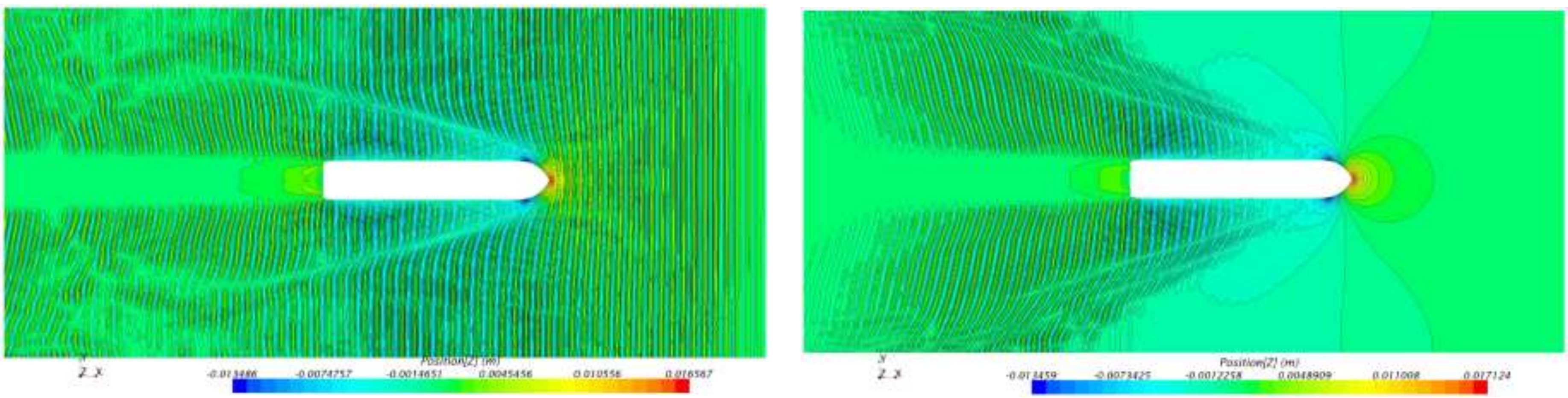

Fig. 5. Numerical damping on STAR-CCM+, where no numerical damping affects the true waves generated by the inland vessel (left), unlike numerical damping with length of 9 m applied only at inlet and outlet boundary conditions (right).

Content

4. Empirical models

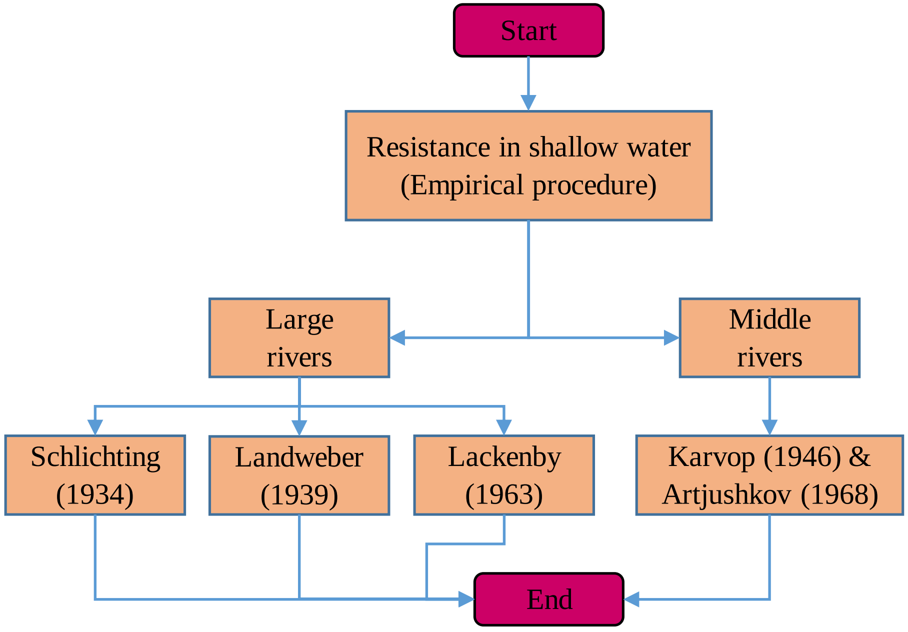

Fig. 6. Empirical procedure.

Content

5. Methodology

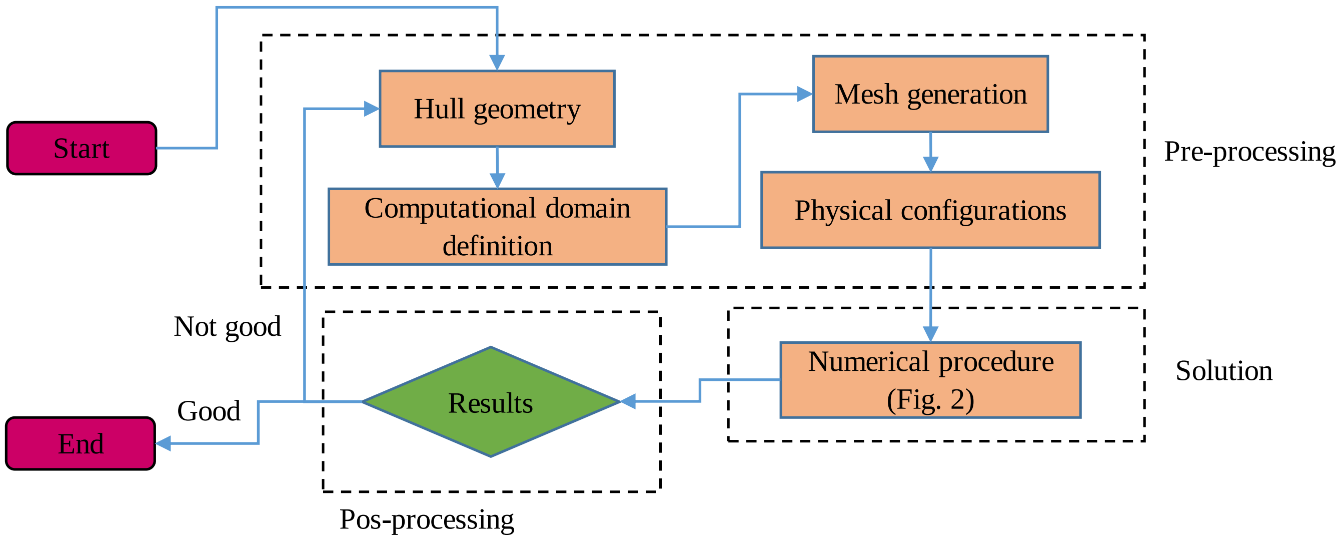

Fig. 7. Numerical procedure.

5. Methodology

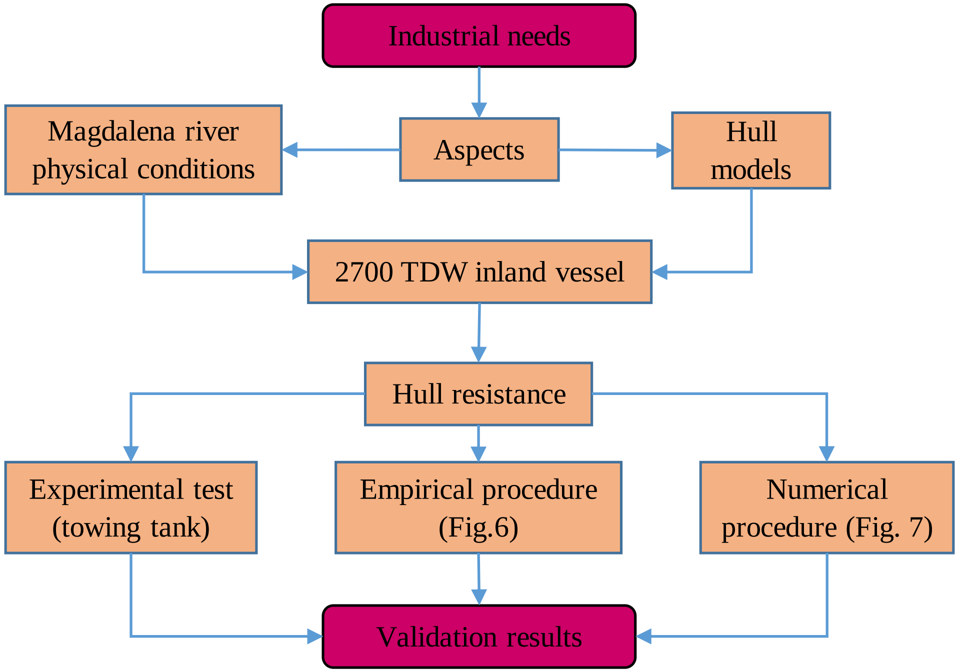

Fig. 8. General methodology.

Content

6. Results

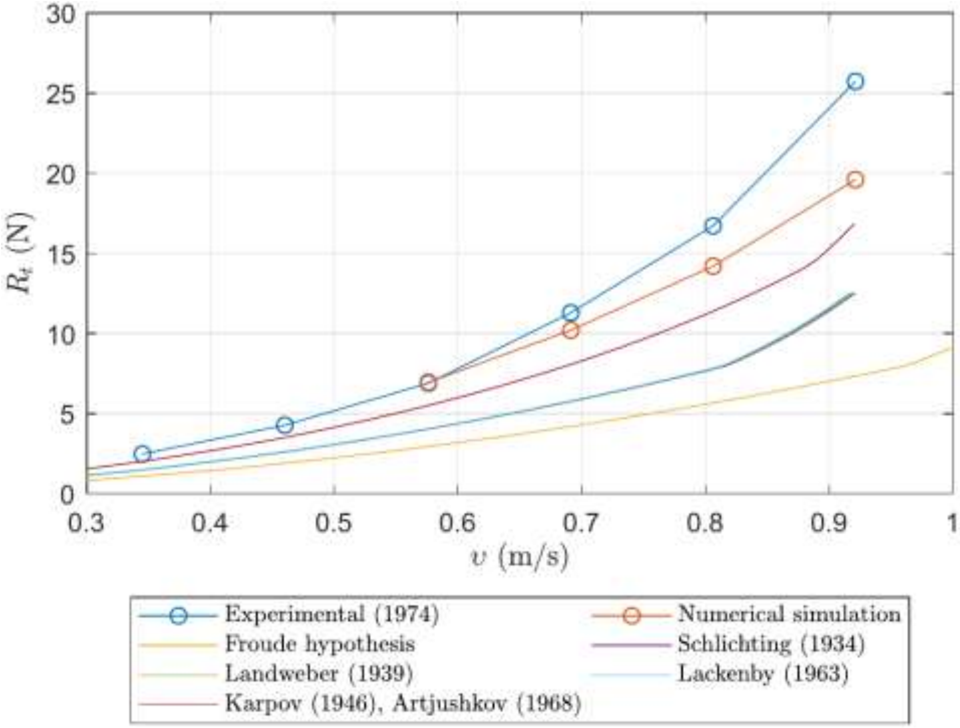

Fig. 9. Comparison of methods with 2700 TDW inland vessel.

v (m / s)	R_t (N) Experimental	CFD	Empirical	E_r (%) CFD	Empirical
0.576	6.89	6.96	5.59	-1.02	18.87
0.691	12.29	10.20	8.00	9.65	29.14
0.806	16.71	14.20	11.52	15.02	31.06
0.921	25.72	19.60	16.06	23.80	37.59

Table 3. Comparison of numerical and numerical methods with experimental results.

6. Results

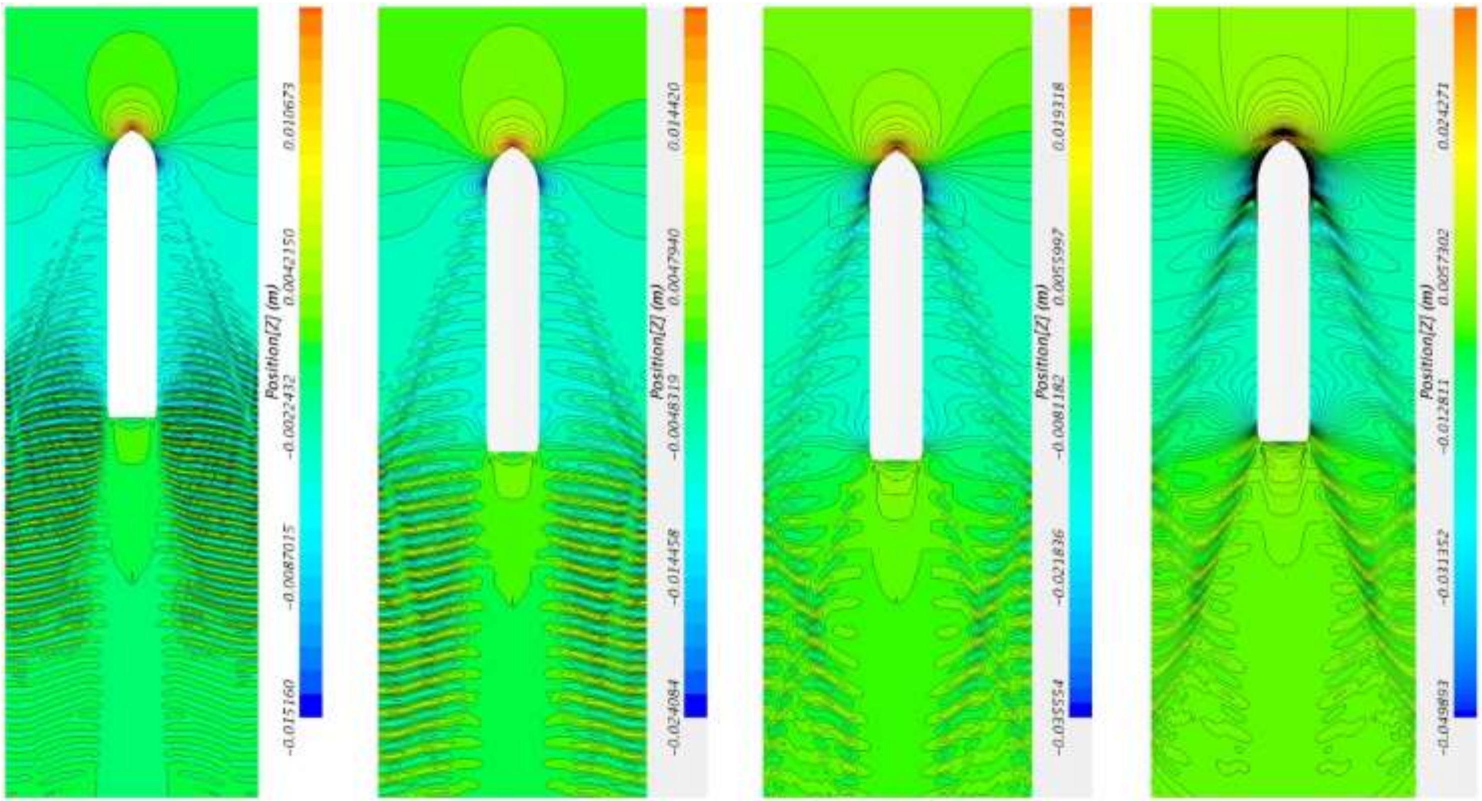

(a) $v = 0.576$ (b) $v = 0.691$ (c) $v = 0.806$ (d) $v = 0.921$

Fig. 10. Wave patterns generate by 2700 TDW self-propelled inland vessel.

6. Results

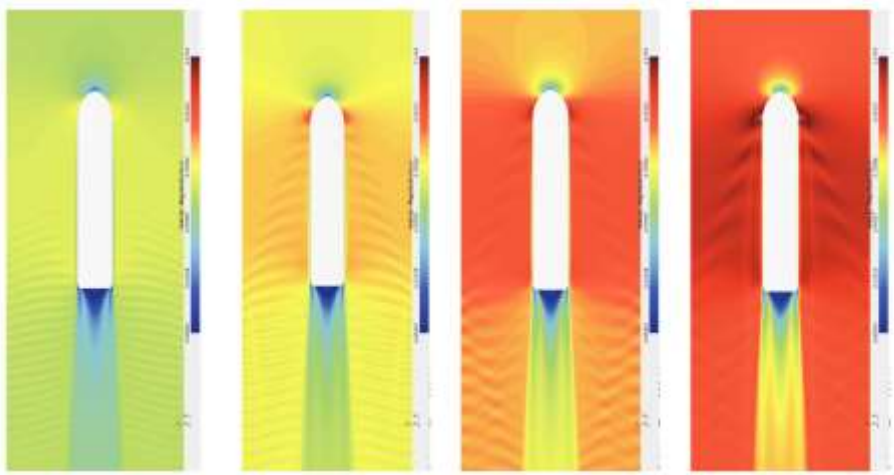

(a) Max v = 0.77472 m/s at 0.576 m/s (b) Max v = 0.94712 m/s at 0.691 m/s (c) Max v = 1.0793 m/s at 0.806 m/s (d) Max v = 1.1764 m/s at 0.921 m/s

Fig. 11. Velocity distribution generated by 2700 TDW inland vessel in top view.

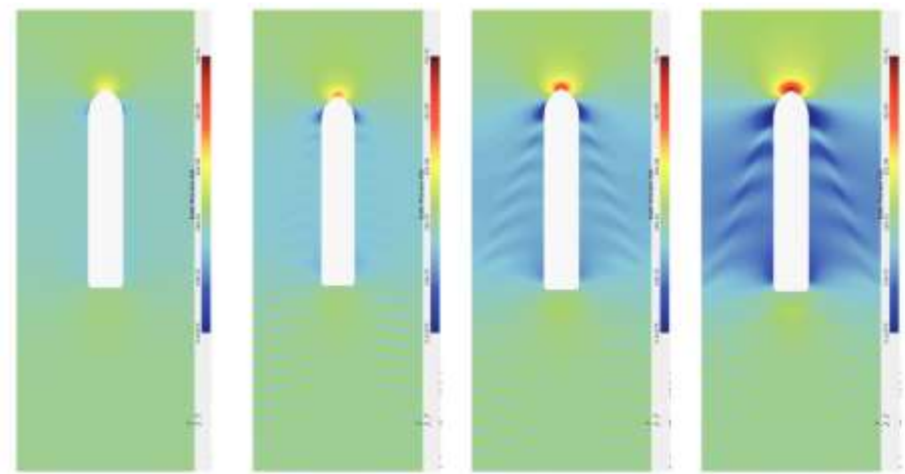

(e) Min p = 144.63 Pa, Max p = 455.77 Pa at 0.576 m/s (f) Min p = 58.274 Pa, Max p = 525.56 Pa at 0.691 m/s (g) Min p = 0.47628 Pa, Max p = 607.50 Pa at 0.806 m/s (h) Min p = 0.32479 Pa, Max p = 702.41 Pa at 0.921 m/s

Fig. 12. Distribution of the static pressure generated by 2700 TDW inland vessel in top view.

6. Results

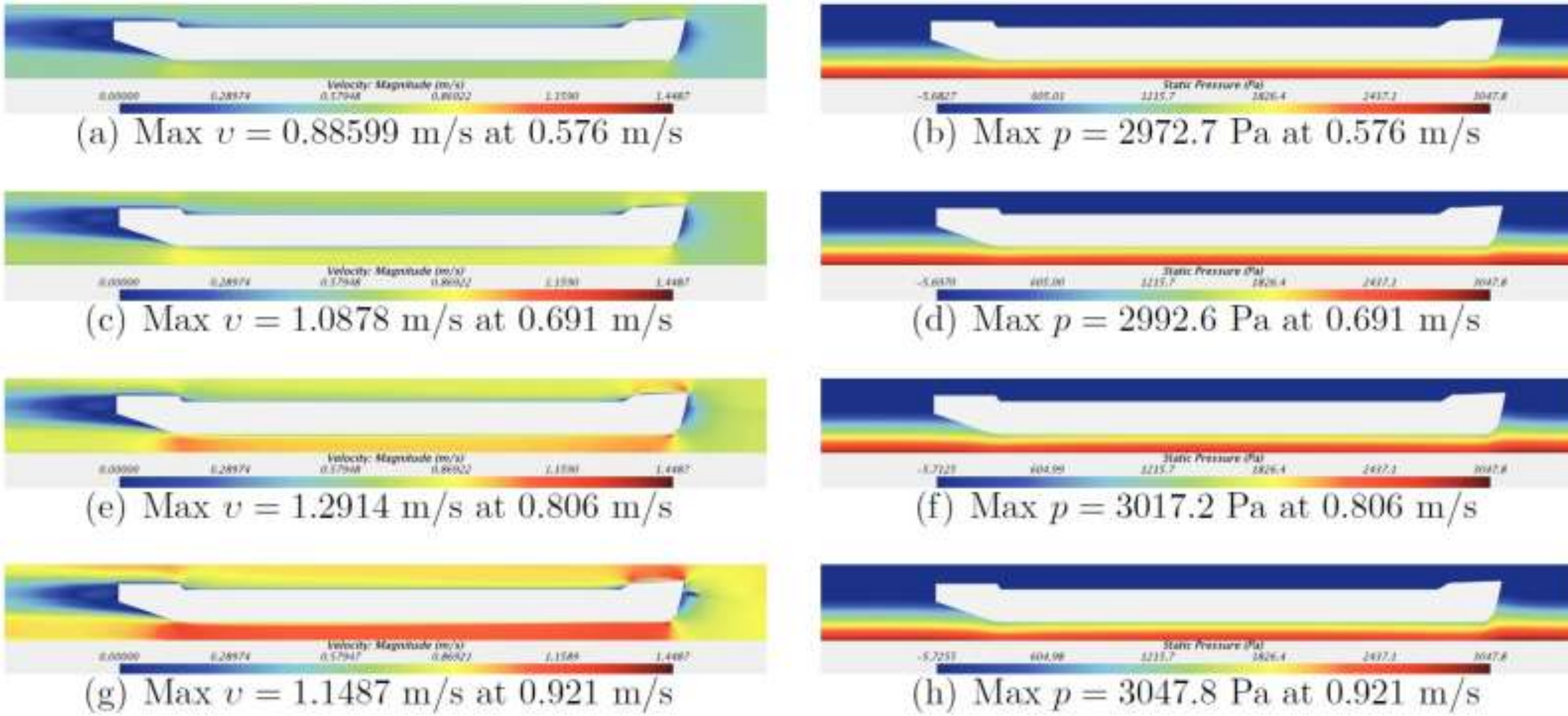

Fig. 13. Velocity and static pressure distribution generated by 2700 TDW inland vessel in symmetric view.

Content

1. Introduction
2. Ship geometry
3. Numerical model
4. Empirical models
5. Methodology
6. Results
7. Conclusions and future works

7. Conclusions and future work

- The formulations for the empirical methods procedure are satisfactory only in case of vessel navigating in middle rivers.
- The numerical simulations are satisfactory only in case of low velocities. As the speed increases, the relative error also increases up to 18%.
- The numerical simulation results can be corrected with more precision.

7. Conclusions and future work

7.1. Future analysis

- Improve the numerical simulation results.
- Calculate convergence criteria by Grid Convergence Index (GCI) developed by Roache (1998) and described by Celik et al. (2008).
- Calculate and illustrate the pressure coefficient, skin friction coefficient and the dimensionless wall $y+$ of the hull.

Colombia
mar2019